29 p.

N64 13270
CODE-1
CR-53014

Technical Report No. 32-364

Optical Free-Flight Wake Studies

Bain Dayman, Jr.

OTS PRICE

XEROX $ 2.60 ph.

MICROFILM $ 1.07 mf.

jpl

JET PROPULSION LABORATORY
CALIFORNIA INSTITUTE OF TECHNOLOGY
PASADENA, CALIFORNIA

November 1, 1962

NATIONAL AERONAUTICS AND SPACE ADMINISTRATION
CONTRACT NO. NAS 7-100

X OTS
2

(NASA CR-53014; JPL-TR-32-364) OTS: $2.60 ph, $1.07 mf

Technical Report No. 32-364

Optical Free-Flight Wake Studies

Bain Dayman, Jr.

Robert E. Covey

Robert E. Covey, Chief
Aerodynamic Facilities Section

JET PROPULSION LABORATORY
CALIFORNIA INSTITUTE OF TECHNOLOGY
PASADENA, CALIFORNIA

November 1, 1962

29 p ref

Copyright © 1963
Jet Propulsion Laboratory
California Institute of Technology

CONTENTS

FIGURES

FIGURES (Cont'd)

PREFACE

This Report represents one phase of research performed at the Jet Propulsion Laboratory, California Institute of Technology, sponsored by the National Aeronautics and Space Administration under Contract NAS 7-100. With the exception of Part IV, all material is included in the Anti-Missile Research Advisory Council (AMRAC) Proceedings (published by the University of Michigan) of the November 1962 meeting in Philadelphia, Pa.

ABSTRACT

In conjunction with the extensive effort being put into the determination of wake properties, a program has been initiated in the supersonic and hypersonic wind tunnels at the Jet Propulsion Laboratory (JPL) to obtain spark schlieren photographs of the separation and near-wake regions of various free-flight (no support interference) bodies. The purpose of this Report is to present the technique used at JPL along with typical examples of the photographic data, in order to make it possible to evaluate the procedures used and information obtained by free-flight testing in a conventional wind tunnel, in complement with the large variety of experimental work now in progress. For the most part, the models investigated were of two types, spheres and 30-deg included-angle cones.

I. INTRODUCTION

Much interest has recently been shown by experimenters and theoreticians with regard to the problem of entry-vehicle wakes. The gathering of definitive model wake pictures under free-flight conditions is an expensive and time-consuming process. At the Jet Propulsion Laboratory (JPL), the technique of simplified free-flight testing (Ref. 1) in supersonic and hypersonic wind tunnels (Ref. 2) is being developed. This type of testing greatly enhances the opportunity for obtaining large amounts of photographic data of free-flight model wakes in a short period of time.

During the development of this free-flight technique, spark schlieren photographs have been obtained of sphere and cone model wakes in the supersonic wind tunnel through the Mach number range of $1.3 < M < 5$, at varying Reynolds numbers. In addition to free-flight wake pictures, schlieren photographs of model wakes were taken while the models were supported on wires. All of the nonsphere free-flight models were released at zero angle-of-attack and yaw. The intent was to obtain spark schlieren pictures with the models still aligned with the flow direction after about 5 in. of travel. Except for the included yawed model photo, this intent was realized on every flight, i.e., the models were aligned with the flow to within several deg.

The optical windows used in the supersonic wind tunnel for most of the sphere-wake data were of high quality, and except for several chips on the inner window surfaces, there was no apparent optical disturbance. However, the windows used for the cone-wake studies were of inferior optical quality, and striations are quite noticeable in the schlieren photographs. These striations confuse the wake patterns, and must be taken into consideration when the data are analyzed.

The effect of wind-tunnel flow and boundary-layer noise (Ref. 3) upon the model wakes is not known, but must be considered to exist. Any facility which accelerates a gas in order to create the proper environment over the model, has noise in the flow which impinges directly upon the model and the wake. To what degree this noise affects the wake properties (such as when the wake transists to turbulent and the turbulent nature) must be determined before wake data obtained in a wind tunnel can be considered indicative of the conditions of an actual flight vehicle.

II. GENERAL DESCRIPTION OF TESTING TECHNIQUE

A. Supersonic Wind Tunnel ($1.3 < M < 5.5$)

The model to be investigated is supported at the upstream end of the test section window on a vertical wire. A typical test installation is shown in Fig. 1. This wire (0.020 to 0.024-in. D) is notched (0.005 to 0.010 in.) within the model. Once the proper test section flow conditions have been established, this preloaded wire (30 to 70 lb) is broken at the notch. This is accomplished by the application of an impulse load (10 to 30 lb) at one end of the wire, outside the tunnel. The breaking of the wire triggers a circuit which fires a spark source (3 μsec duration) at a desired time delay in order to obtain a schlieren picture of the model in flight. A fairly complete description of this technique appears in Ref. 1.

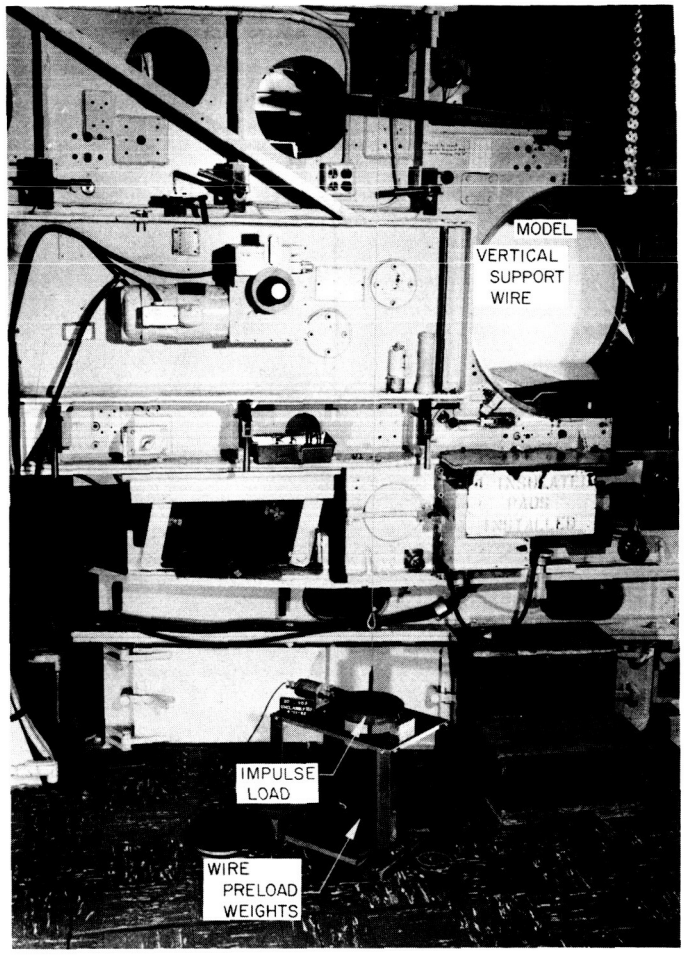

Fig. 1. Test installation — supersonic wind tunnel

B. Hypersonic Wind Tunnel ($4 < M < 11$)

The model support and release procedures are virtually the same as those used in the supersonic wind tunnel. However, several additional test conditions are possible. The model wall temperature can be varied from approximately that of liquid nitrogen ($-350°$ F) to an adiabatic condition, and the total tunnel temperature can be as high as 1300° F at all Mach numbers. However, as the Mach number is increased above $M = 5$, the wake definition with the schlieren system rapidly falls off, and is totally inadequate at $M > 7$. At high Mach numbers, and at low Reynolds numbers, a satisfactory method of flow ionization is used for observing the wake details. (Ref. 4.)

III. FREE-FLIGHT CONE WAKES (SUPERSONIC WIND TUNNEL)

The 1½-in. D cones, which weighed about 5 g, were molded from polyurethane foam, and then ballasted with enough lead to keep the model-flight accelerations below 100 g's, and to put the center of gravity sufficiently ahead of the center of pressure. As it was not convenient to cast these cones with fine points, the cone tips were truncated, leaving a flat surface parallel to the cone base of approximately 0.03-in. D.

Spark schlieren photographs of the free-flight cones (30 deg included-angle) were obtained through the Mach range of $1.5 < M < 4.6$. At $M = 1.6$, the Reynolds number was varied through a factor of 8. Figure 2 reveals the separation and near-wake regions through the Mach number range at the maximum Reynolds number condition (1-in. grid spacings were used). The onset of wake turbulence can easily be seen at $M = 1.6$ and 2, and is certainly discernable for the other Mach numbers. The somewhat poor quality of the $M = 3$ picture is due to double exposure, once with the model in position, and again with no model in the test section (the model was blackened in an attempt to make this picture conform with the set). The downstream travel of the wake throat with increasing Mach number is quite apparent in the graphic illustration. The measurement of lengths such as L' are speculative and are intended only for qualitative use. This distance is from the base of the cone to where the separation region is asymptotic to the wake.

The effect of Reynolds number variation upon the free-flight cone wakes was investigated at $M = 1.6$. The minimum freestream Reynolds number (based upon the cone diameter) was limited by the sensitivity of the schlieren system. In Fig. 3, as R_D was decreased to 2×10^5 from the maximum of 8×10^5, the diameter of the wake throat decreased. This diameter then increased as the Reynolds number was further decreased to $R_D = 1 \times 10^5$. However, the subjective distance L' appears to be relatively invarient with the change in Reynolds number.

Normally, the model boundary layers were laminar. However, at $M = 1.6$ and 2, the model boundary layers were made turbulent by use of 0.010-in. D wire trip rings (Ref. 5), located approximately 0.38 in. from the cone tip. The turbulent portions of the free-flight cone wakes of the laminar boundary layer models appear to be more vigorous than for the turbulent boundary layer models (Fig. 4). An enlarged picture of the $M = 2$ models in flight (Fig. 5) clearly indicates a laminar model boundary layer with no trip. With a trip ring, the laminar boundary layer transits to turbulent at approximately 60% of the distance from the nose to the base.

Although approximately one flight in ten was considered unsuccessful, even these provided information of some interest. An example of one such "misfire" is that of a cone model which yawed at 30 deg (estimated from the base "bulge") at the time the spark schlieren picture was taken (Fig. 6). The neck of the wake appears to be narrower in the yawed case than in that with no yaw.

The effect on the cone wake due to nose blunting (nose radius to base diameter ratio of 0.10) was investigated at $M = 4$. Figure 7 shows the effect of a 0.030-in. D wire trip ring on the blunted cone. Without trip, the blunting had little effect upon the wake shape. With trip, the effect was quite impressive. Even in these rather small reproductions of the spark schlieren photographs, the effect of the trip upon the model boundary layer is easily seen: the boundary layer is substantially thickened and is turbulent.

The hole through each model had to be large enough to minimize any motion imparted to the model upon the breaking of the wire. Therefore, the cones were held in the proper position on the vertical wire by use of locating tags (Fig. 8). Investigations were not made of the effects of just the vertical wire upon the cone wakes, as these tags were used on every run. In order to make it possible to run without the locating tags, and because of the time factor involved, no runs were made with tight holes in the models. Comparison of the model wakes (still supported on the wire with the free-flight wakes) indicated that for $M \leq 2$ there was negligible effect of the support upon the wakes, while for $M > 2$, the effects of the wire support upon the wakes became larger with increasing Mach numbers. The interference effect of the wire support decreases the characteristic length (L') of the wake (Fig. 9).

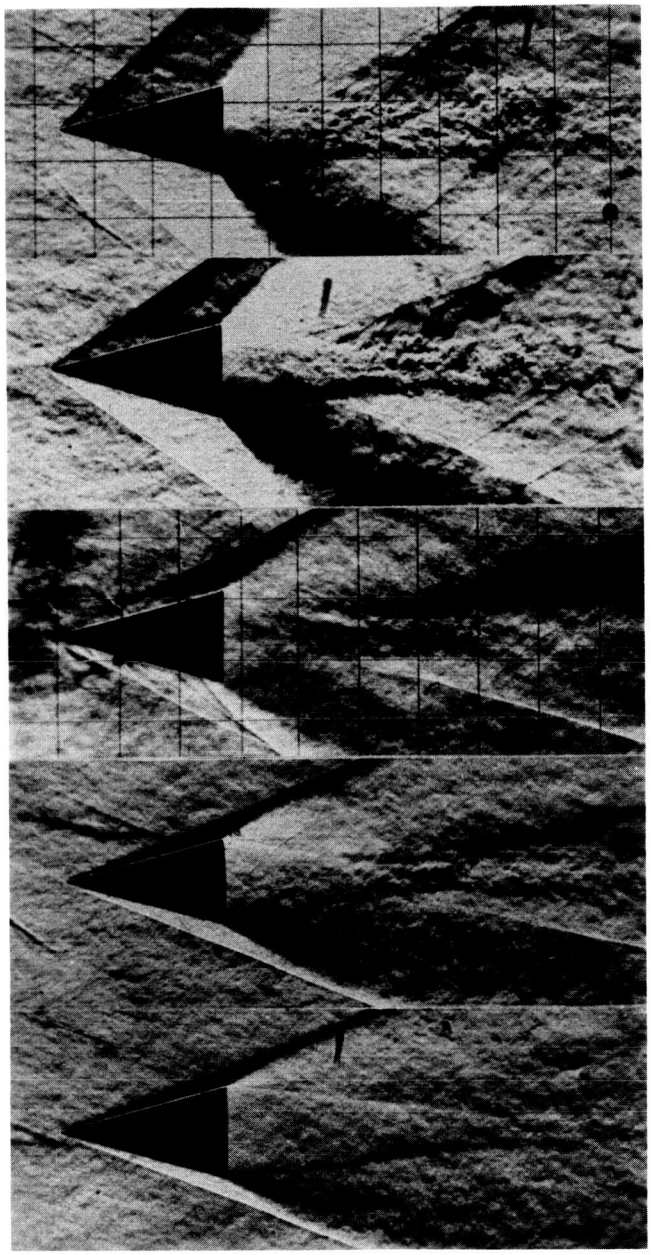

MACH NO.	SUPPLY PRESSURE, cm Hg	R_D
1.58	120	8×10^5
1.92	140	8×10^5
2.99	150	5×10^5
3.92	250	5×10^5
4.64	330	$4\frac{1}{2} \times 10^5$

30-deg APEX ANGLE
$1\frac{1}{2}$-in. D BASE
LAMINAR MODEL BOUNDARY LAYER

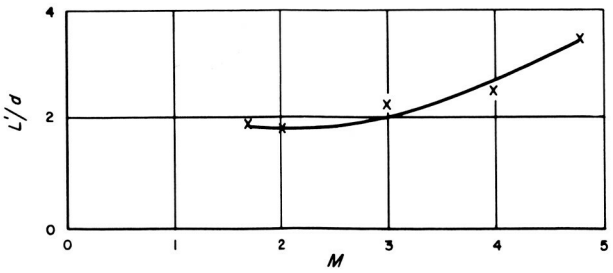

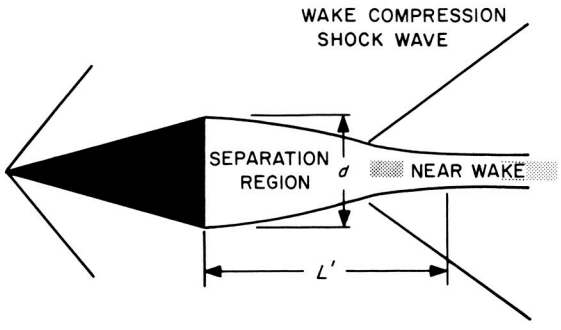

Fig. 2. Effect of Mach number on free-flight cone wakes

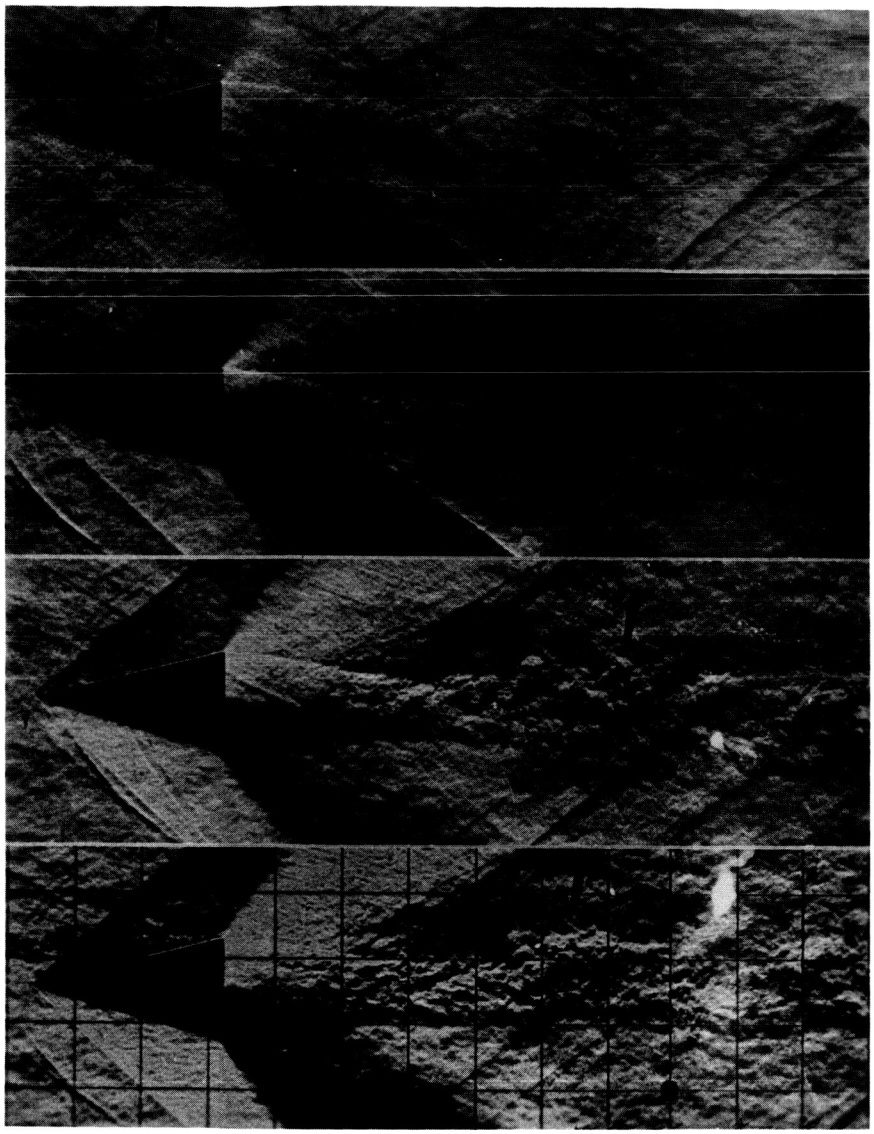

SUPPLY PRESSURE, cm Hg	R_D
15	1×10^5
30	2×10^5
60	4×10^5
120	8×10^5

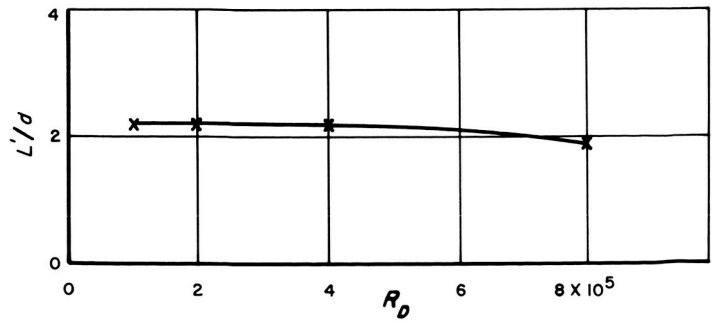

$M = 1.58$
30-deg APEX ANGLE
$1\frac{1}{2}$-in. D BASE
LAMINAR MODEL BOUNDARY LAYER

Fig. 3. Effect of Reynolds number on free-flight cone wakes

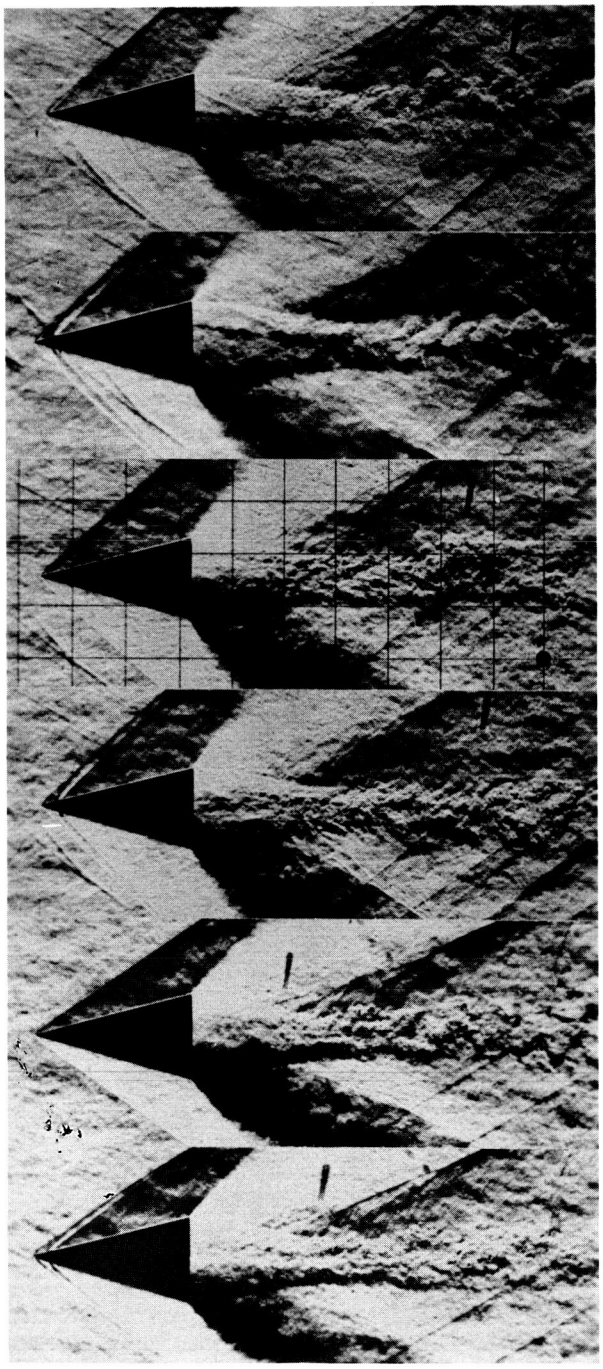

MODEL BOUNDARY LAYER	MACH NO.	SUPPLY PRESSURE, cm Hg	R_D
LAMINAR	1.61	60	4×10^5
TURBULENT	1.61	60	4×10^5
LAMINAR	1.58	120	8×10^5
TURBULENT	1.58	120	8×10^5
LAMINAR	1.92	140	8×10^5
TURBULENT	1.93	140	8×10^5

30-deg APEX ANGLE
$1\frac{1}{2}$-in. D BASE

Fig. 4. Effect of model boundary layer on free-flight cone wakes

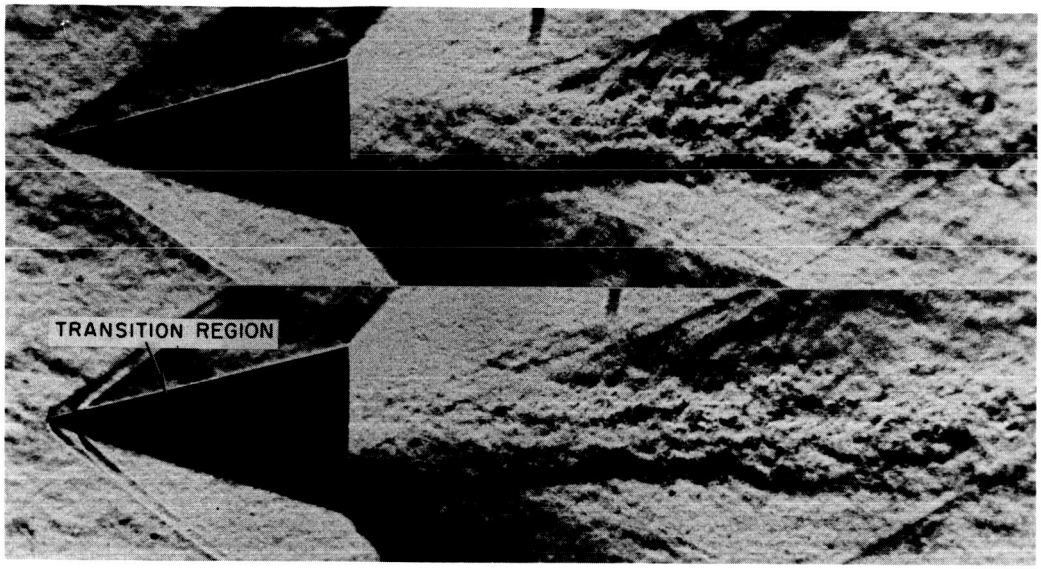

NO TRIP RING:
LAMINAR BOUNDARY
LAYER ON CONE

0.010-in. D TRIP RING:
BOUNDARY LAYER
TRANSITION ON CONE

$M = 2$, SUPPLY PRESSURE = 140 cm Hg, $R_D = 8 \times 10^5$
30-deg APEX ANGLE, $1\frac{1}{2}$-in. D BASE

Fig. 5. Effect of wire trip ring on free-flight cone boundary layer and wake

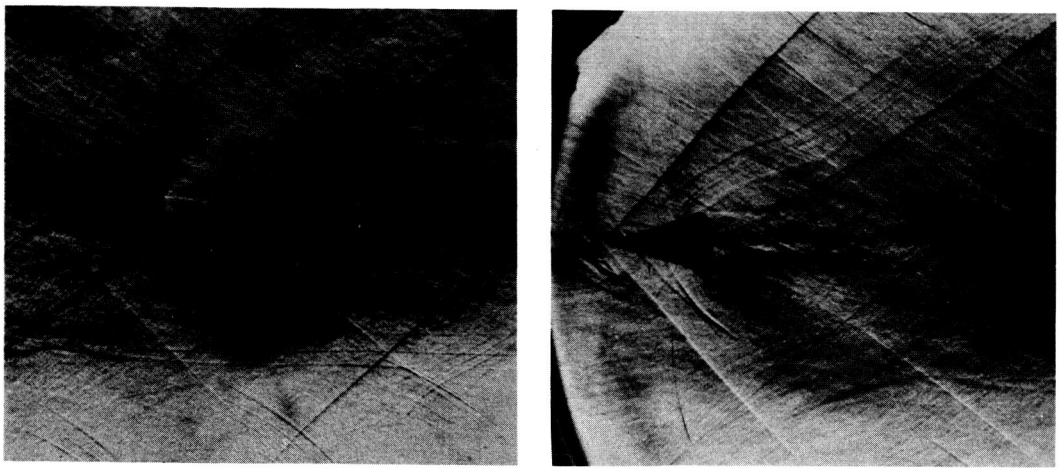

YAW = 0 deg

YAW ≈ 30 deg

$M = 1.57$
SUPPLY PRESSURE = 15 cm Hg
$R_D = 1 \times 10^5$
30-deg APEX ANGLE
$1\frac{1}{2}$-in. D BASE
LAMINAR MODEL
BOUNDARY LAYER

Fig. 6. Effect of yaw angle on free-flight cone wakes

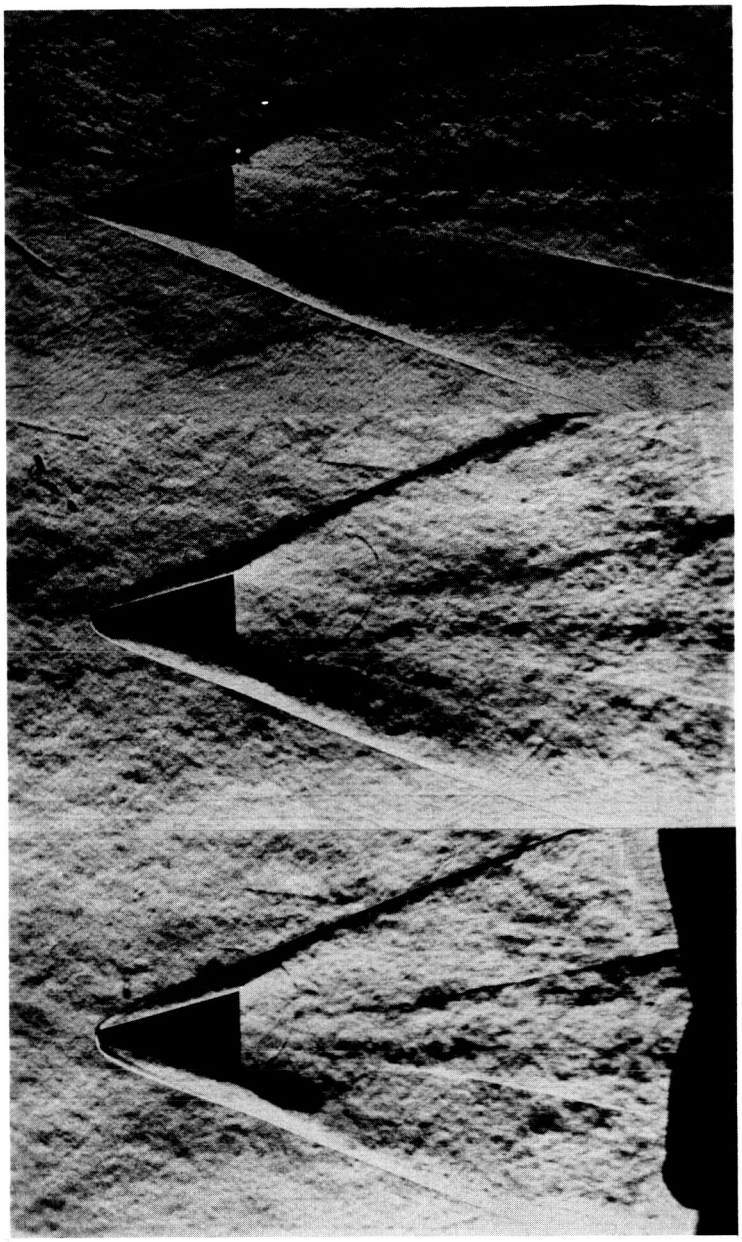

$\frac{r}{d}$

0

0.1

0.1

0.030-in. D
WIRE TRIP RING

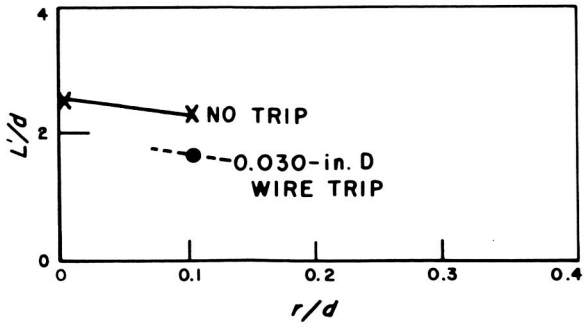

$M = 3.8$
SUPPLY PRESSURE = 250 cm Hg
$R_D = 5 \times 10^5$
30-deg APEX ANGLE
$1\frac{1}{2}$-in. D BASE

Fig. 7. Effect of nose bluntness on free-flight cone wakes

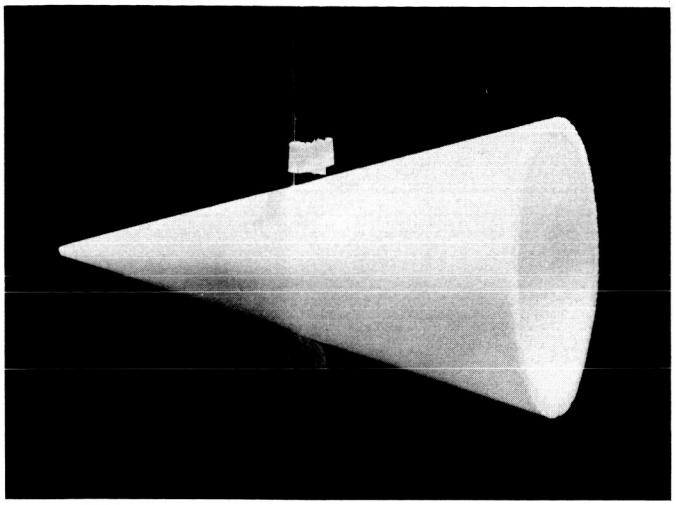

Fig. 8. Photograph of foam cone model on vertical wire support

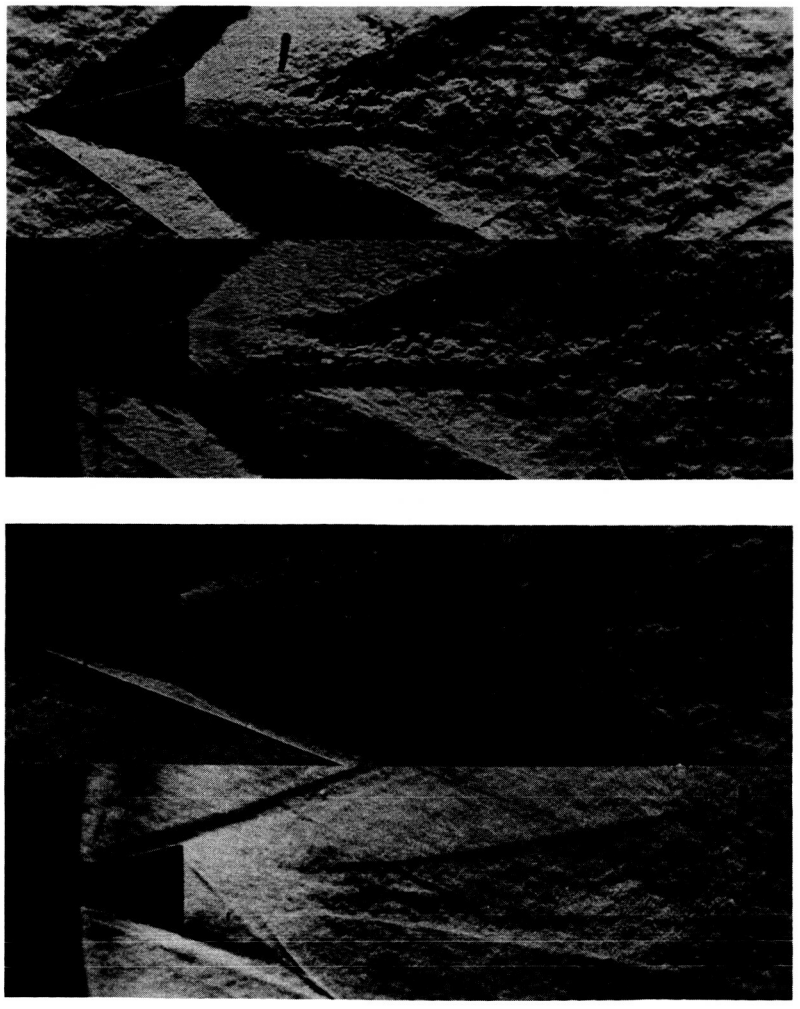

	MACH NO.	SUPPLY PRESSURE, cm Hg	R_D
FREE-FLIGHT	1.92	140	8×10^5
WIRE-SUPPORTED	2.02	140	8×10^5
FREE-FLIGHT	4.64	330	$4\frac{1}{2} \times 10^5$
WIRE-SUPPORTED	4.77	330	$4\frac{1}{2} \times 10^5$

30-deg APEX ANGLE
$1\frac{1}{2}$-in. D BASE

Fig. 9. Effect of wire support on cone wakes

IV. FREE-FLIGHT CONE WAKES (HYPERSONIC WIND TUNNEL)

The flow-ionization technique was used to obtain cone wake pictures at $M = 9$, because the normal schlieren system is not sensitive enough under such conditions. The test installation for observing wakes of free-flight models by means of flow-ionization is shown in Fig. 10. The flow region behind the model is ionized by passing dc current from the probe tip, above the model, to the grounded rod below. The probe tip is insulated with ceramic on the leading edge and top portions, in order to direct the ionization downward. The insulated probe holder is conical in order to create a high pressure region downstream of the tip, and thereby minimize the current leakage around the holder. As can be seen in Fig. 11, the ionized flow region is limited to that region between the probe and the grounding rod.

The model is suspended on a notched wire, which is insulated from ground so as to minimize the tendency of the probe to arc to the wire. The shield in front of the model is used for cooling purposes; gaseous nitrogen, blown over an aluminum model, will cool it to 0° F, while liquid nitrogen will cool it to −350° F. The model is released into flight approximately one sec after the shield is raised out of the way. Motion pictures can be taken of the ionized flow field, the camera being started just prior to release of the model. The two pictures of the flow field in Fig. 11 are consecutive frames taken at 64 frames/sec. The top picture shows the cone model suspended on the wire, while the lower picture shows the model in flight.

Black and white film does not adequately distinguish between the various blue and purple shades of the ionized flow patterns, and it is recommended that high-speed color film be used. The pictures shown in Fig. 11 are black and white copies from the color films, and do not retain the high-quality wake pattern definition of the color film. Although free-flight wake data has been obtained for several cone shapes, at various wall temperatures, and through a range of Reynolds numbers, examples of only one condition are included in this Report. This is due to the lack of wake detail in the black and white reproductions of the color pictures.

The extremely large interference effects of the 0.024-in. D wire support on the flow pattern can be seen in Fig. 11. Although the wake in the lower picture is free

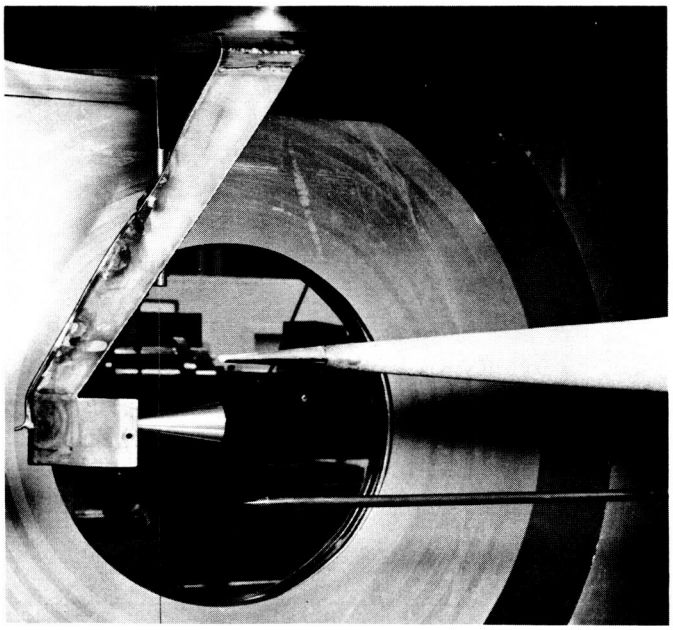

Fig. 10. Test installation — hypersonic wind tunnel

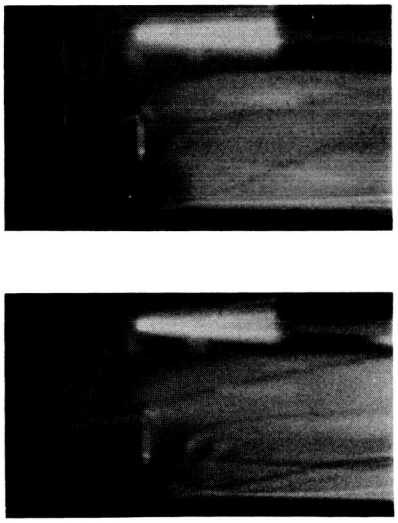

Fig. 11. Example of cone wake patterns as indicated by ionized flow

from any support interference, it is not necessarily an undisturbed wake due to the impingement of the grounding-rod bow shock-wave on the wake at approximately three diameters aft of the model base. In practice, the free-flight model should be located midway between the probe and grounding rod, and it should be smaller in relation to the distance between the probe and grounding rod than indicated in this example.

The exact significance of the various shades of blue and purple in the ionized wake is not known, but the general shape of such a color-outlined wake appears to be in keeping with the shape observed by the normal schlieren technique. Although the slight amount of ionization required to make the flow patterns visible does not usually affect the basic flow patterns, such has not yet been proven for the wake. Investigations of interference-free, two-dimensional wakes will be required before a definite conclusion can be reached with regard to the effect of ionization upon the wake shape.

The purpose of presenting an example of an ionized free-flight cone wake in this Report is to indicate that such data can be obtained, and to compare it with the standard schlieren technique at lower Mach numbers.

V. FREE-FLIGHT SPHERES

In the JPL supersonic wind tunnel, spark schlieren pictures of free-flight spheres were obtained for $1.3 < M < 5$ at various Reynolds numbers. The spheres ranged in size from ½ to 1½-in. D. In general, they were molded from silastic rubber mixed with powdered lead.

Figures 12 and 13 show the effect of Mach number upon the wakes of free-flight spheres at both low and high Reynolds numbers. The variation of the distance L with Mach number is more readily discernible in the case of a high Reynolds number than in that of a low Reynolds number. The distance, L, is very subjective and depends entirely upon the questionable consistency of the person making the measurement. The included

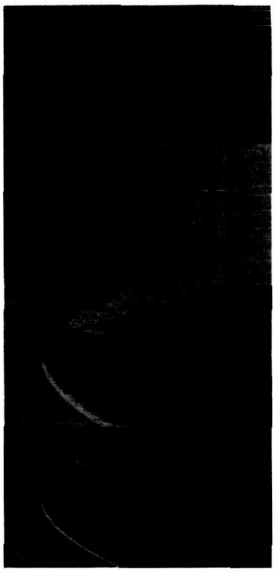

M	MODEL DIAMETER, in.	SUPPLY PRESSURE, cm Hg	R_D
1.3	¾	50	1.8×10^5
1.6	¾	50	1.7×10^5
3	¾	120	2.1×10^5
4	1½	120	2.6×10^5

Fig. 12. Effect of Mach number on free-flight sphere wakes (low Reynolds number)

graph is merely a qualitative interpretation of the schlieren photographic data.

An investigation was made to determine the effect of sphere size on wake shape at both $M = 2$ and 3 (at each Mach number, respectively, the same Reynolds number was used, based upon model diameter). At $M = 2$, except for the picture quality difference due to the need of an extra factor of two enlargements of the smaller sphere, the effect of model size appeared to be insignificant (Fig. 14). However, at $M = 3$, an effect was evident. In Fig. 15, the L/d ratio for the ½-in. D sphere is much smaller than for the ¾-in. D sphere at only a 10% larger model freestream Reynolds number. The cause of this anomaly is not known, and additional studies should be carried out before any conclusions are drawn. These data are presented merely to alert experimenters to the possibilities of inconsistent data. The wake shapes for the ¾ and 1½-in. D spheres at $R_D = 2.2 \times 10^5$ are quite similar. Figure 15 also shows the effect on the wake shape for the same sphere size of several Reynolds numbers at $M = 3$.

The effect of model acceleration on sphere wakes is shown to be negligible in Fig. 16. A ping-pong ball was used in order to obtain the 615 g's acceleration, which is approximately one order of magnitude greater than that for usual conditions.

Figure 17 illustrates the effect of model shape (a 10-deg, half-angle blunted cone, with a nose radius of 0.423 times the base diameter in contrast to a sphere) at $M = 3$. The portions of the wakes between the separation points (base of A'-1 model and one-third diameter from base of sphere) and the wake throat are virtually identical; however, the wake compression shock wave of the sphere is somewhat steeper than that for the A'-1 shape, as the sphere is more blunt in shape.

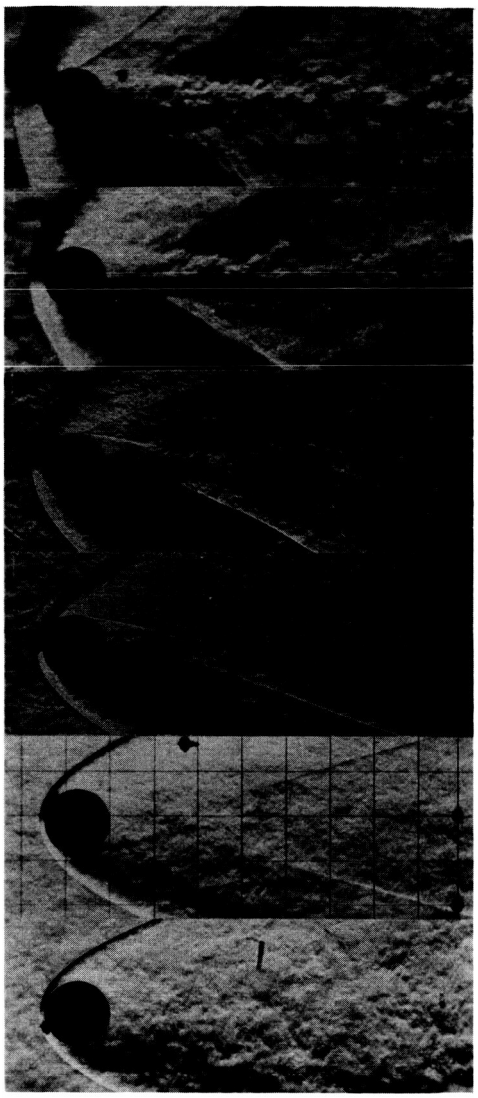

M	MODEL DIAMETER, in.	SUPPLY PRESSURE, cm Hg	R_D
1.3	$\frac{3}{4}$	110	3.8×10^5
1.6	$\frac{3}{4}$	125	3.9×10^5
2	$1\frac{1}{2}$	70	4.0×10^5
3	$1\frac{1}{2}$	162	5.4×10^5
4	$1\frac{1}{2}$	263	5.7×10^5
5	$1\frac{1}{2}$	330	4.2×10^5

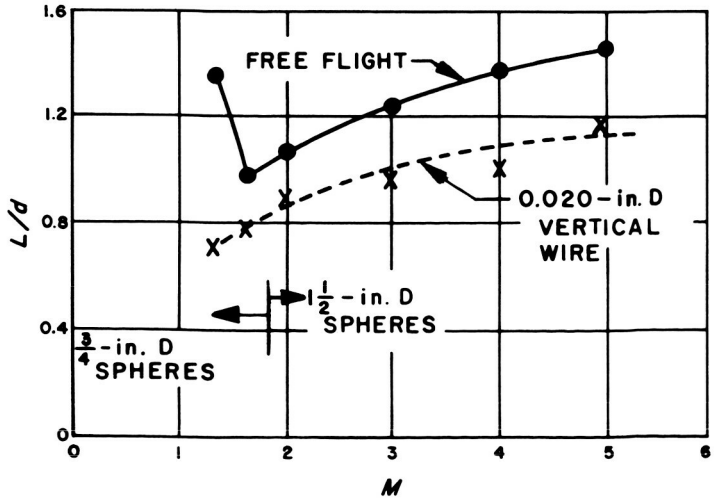

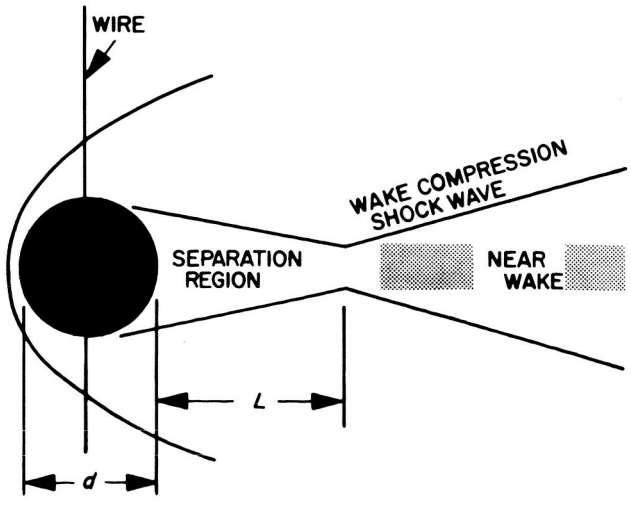

Fig. 13. Effect of Mach number on free-flight sphere wakes (high Reynolds number)

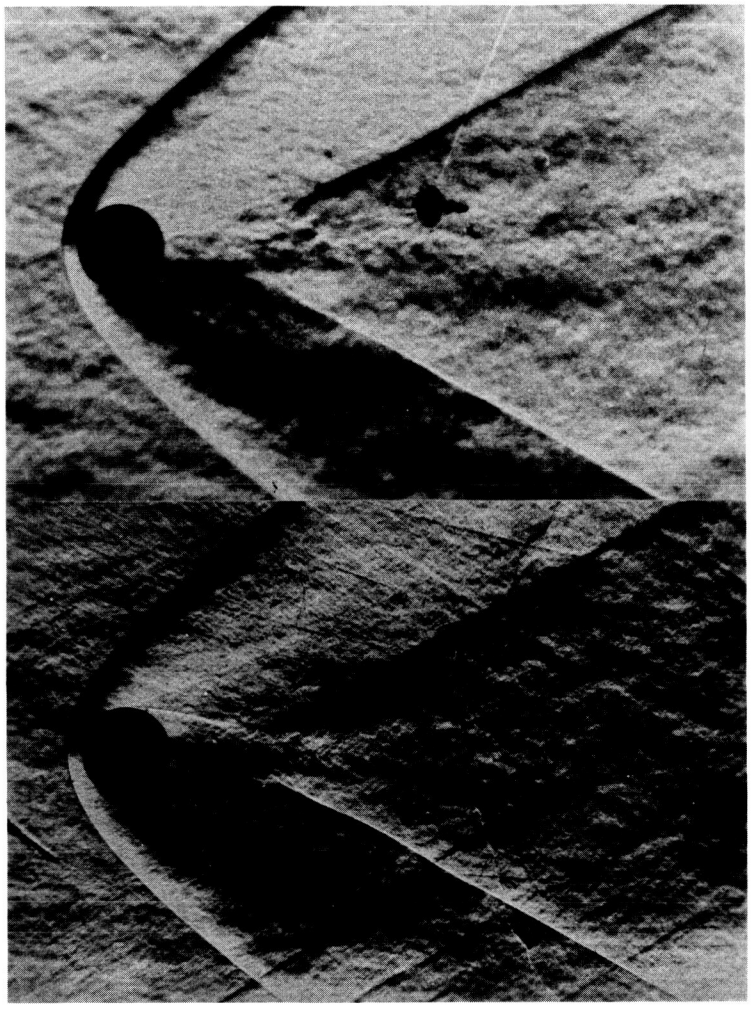

MODEL DIAMETER, in.	SUPPLY PRESSURE, cm Hg	$\frac{L}{d}$
$\frac{3}{4}$	150	0.92
$1\frac{1}{2}$	70	1.04

$M = 2$
$R_D = 4 \times 10^5$

Fig. 14. Effect of model diameter on free-flight sphere wakes

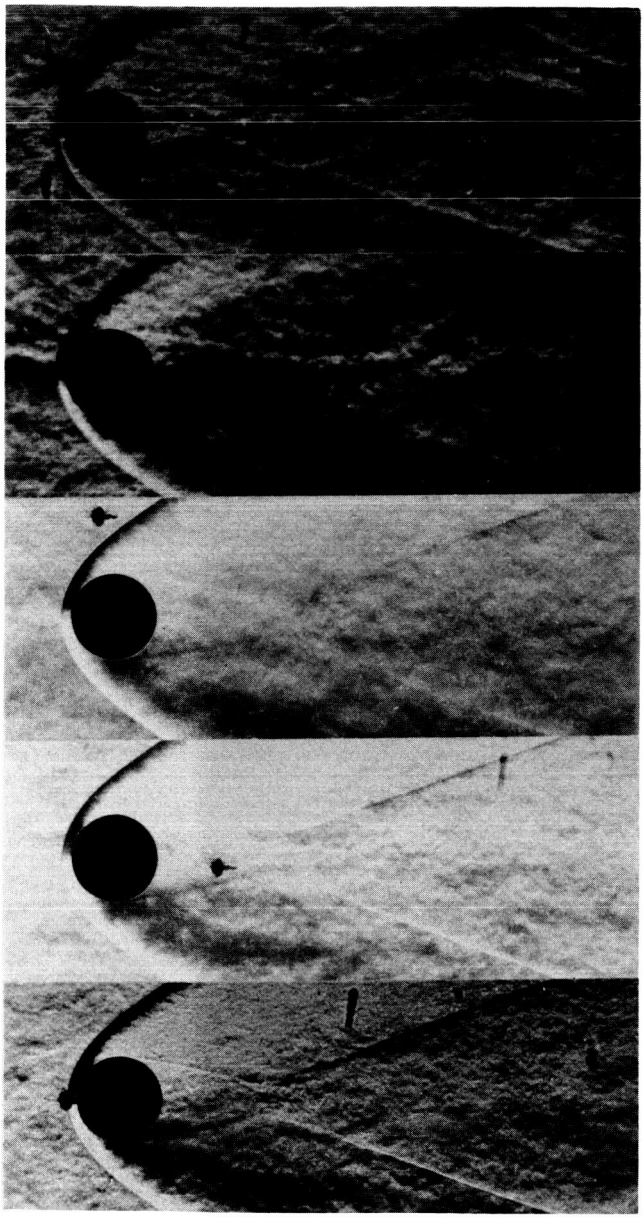

MODEL DIAMETER, in.	SUPPLY PRESSURE, cm Hg	R_D	$\frac{L}{d}$
$\frac{1}{2}$	162	1.9×10^5	1.04
$\frac{3}{4}$	120	2.1×10^5	1.44
$1\frac{1}{2}$	60	2.3×10^5	1.56
$1\frac{1}{2}$	150	5.3×10^5	1.22
$1\frac{1}{2}$	162	5.4×10^5	1.25

$M = 3$

Fig. 15. Effect of Reynolds number and model diameter on free-flight sphere wakes

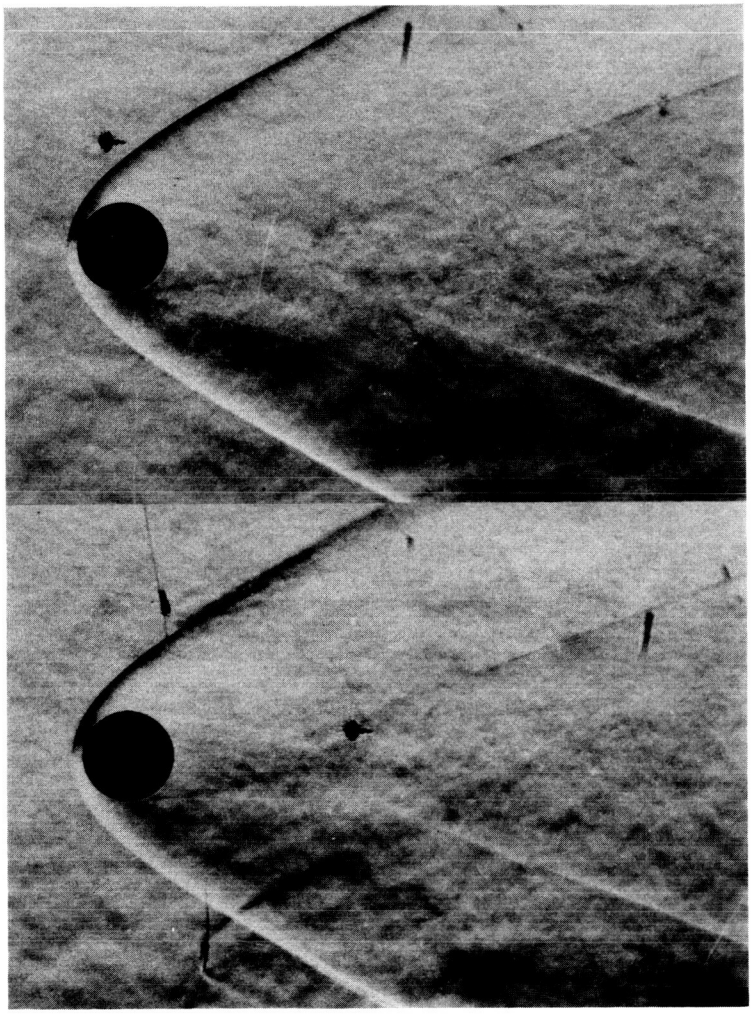

MODEL WEIGHT, gm	MODEL ACCELERATION, g's	$\frac{L}{d}$
$33\frac{1}{2}$	45	1.56
$2\frac{1}{2}$	615	1.56

$M = 3$
SUPPLY PRESSURE = 60 cm Hg
$R_D = 2.2 \times 10^5$
DIAMETER = $1\frac{1}{2}$ in.

Fig. 16. Effect of model acceleration on free-flight sphere wakes

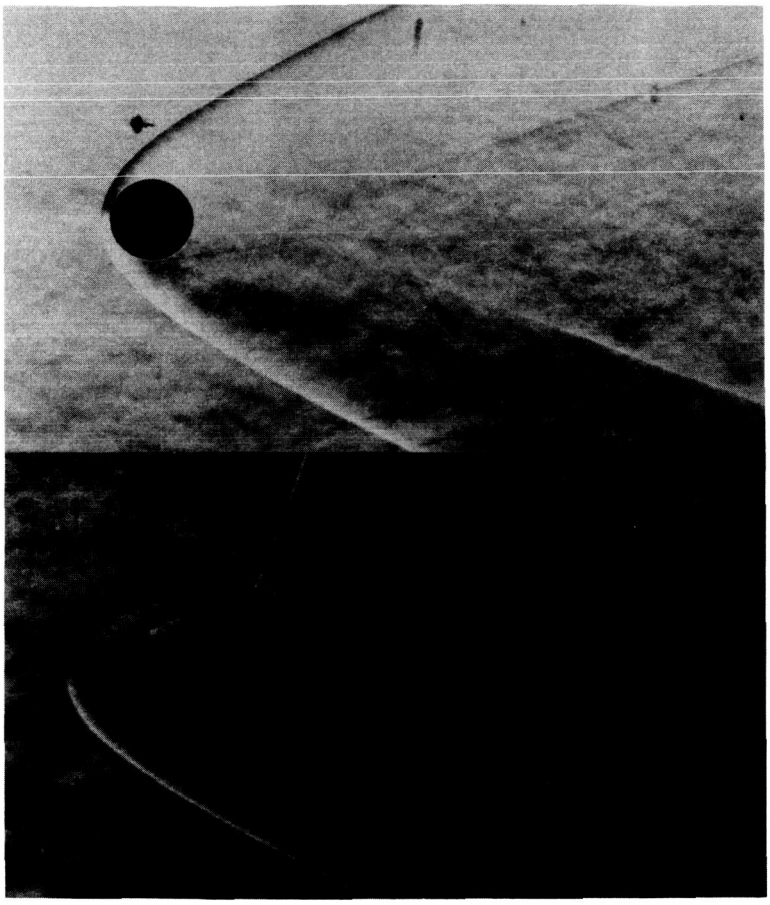

MODEL	DIAMETER, in.	R_D	$\frac{L}{d}$
SPHERE	$1\frac{1}{2}$	2.3×10^5	1.56
$A'-1$	1	1.5×10^5	1.69

M = 3,
SUPPLY PRESSURE = 60 cm Hg

Fig. 17. Effect of model shape on free-flight wakes

VI. SUPPORT-WIRE INTERFERENCE ON SPHERE WAKES

One of the most important facts discovered during these free-flight wake investigations was the appreciable effect even small-diameter wire supports have on the sphere wakes. A fairly thorough study was conducted on the effects of various wire diameters and orientations at $M = 3$. The L/d ratio was found to increase for a wire-supported sphere as the Reynolds number decreases to 0.8×10^5. Figure 18 shows photographic examples of the effect of the vertical wire diameter on the sphere wakes, with a graphical presentation of this and other Reynolds number conditions. The larger the wire diameter, the shorter the length, L, of the separation region. It is clearly indicated that within the realm of test conditions, decreasing the Reynolds number increases the length of the separation region for the smaller diameters of vertical wire supports. The spark schlieren photographs in Fig. 19, at $M = 1.3$ and 1.6, shows the strong effects of a 0.020-in. D wire on the wakes of ¾-in. D spheres. With Fig. 13 is a curve showing the decrease of L/d due to a 0.020-in. D vertical wire from the L/d of the free-flight condition over the Mach number range tested.

Although the effect on the sphere wake L/d for the horizontal wire (0.020-in. D) orientation at $M = 3$ (parallel to the schlieren light path and going through the sphere centerline) appears to be somewhat less than that for the vertical wire, the abundance of shock waves in the photograph makes it difficult to locate the wake pattern (Fig. 20). This spark schlieren photograph serves to emphasize the amount of disturbance a single wire support actually creates, as contrasted to the relatively small disturbance shown in the case of the vertical wire support. In Fig. 20, support is also provided by both horizontal and vertical wires. Similar data at other Reynolds numbers and wire diameters indicate like effects.

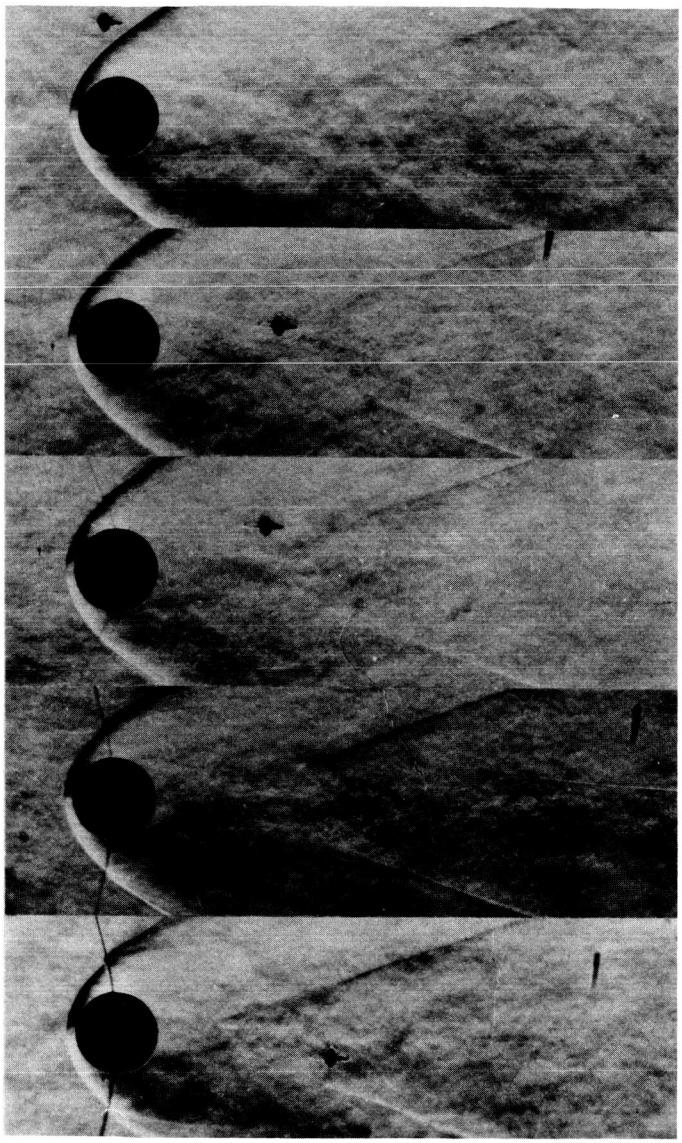

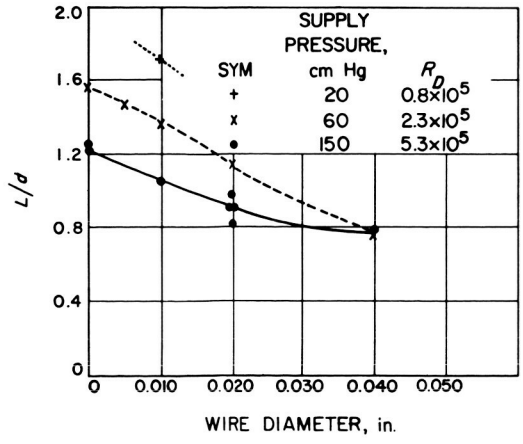

Fig. 18. Effect of diameter of vertical wire support on sphere wakes

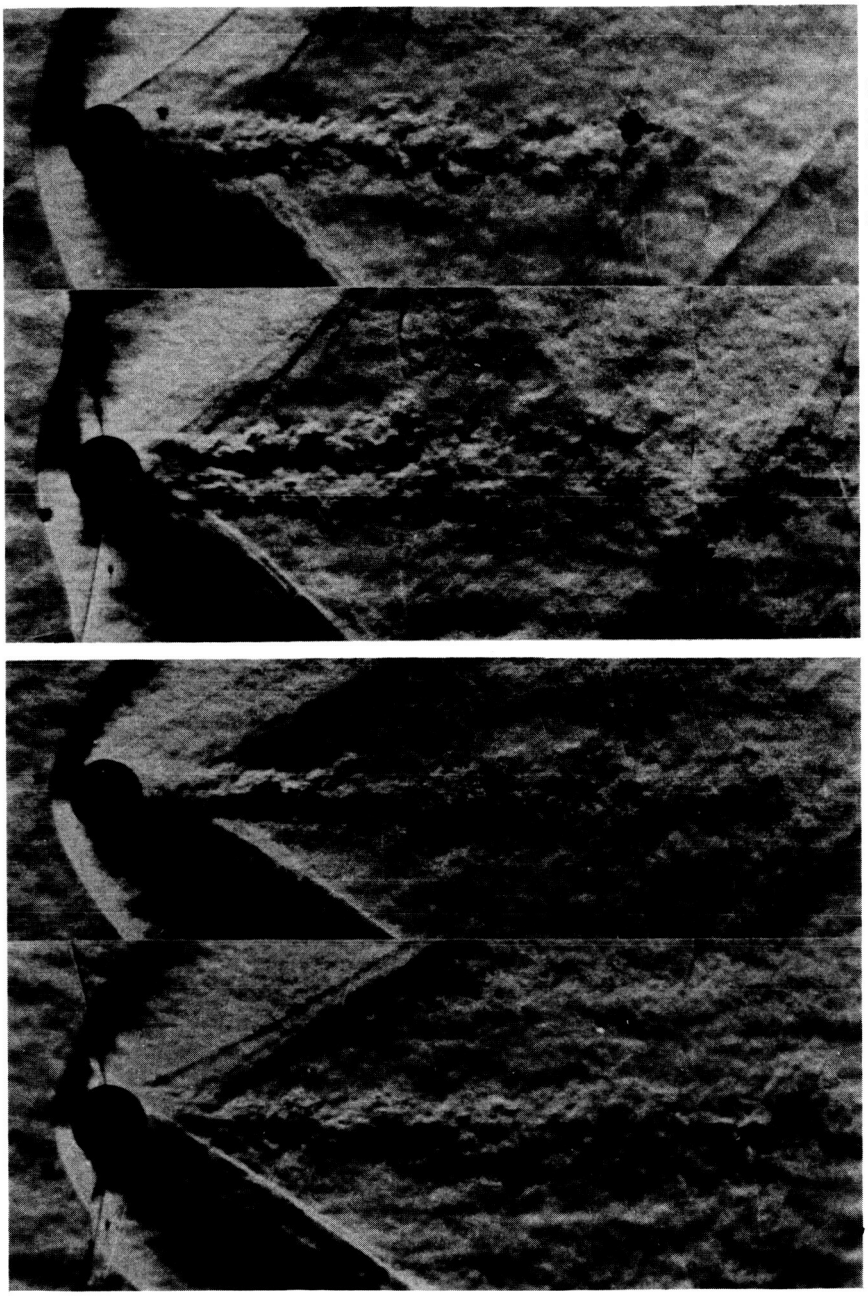

	M	SUPPLY PRESSURE, cm Hg	R_D
FREE-FLIGHT	1.3	110	4×10^5
WIRE-SUPPORTED	1.3	110	4×10^5
FREE-FLIGHT	1.6	125	4×10^5
WIRE-SUPPORTED	1.6	125	4×10^5

$\frac{3}{4}$-in. D MODELS
0.020-in. D WIRE

Fig. 19. Effect of vertical wire support on sphere wakes

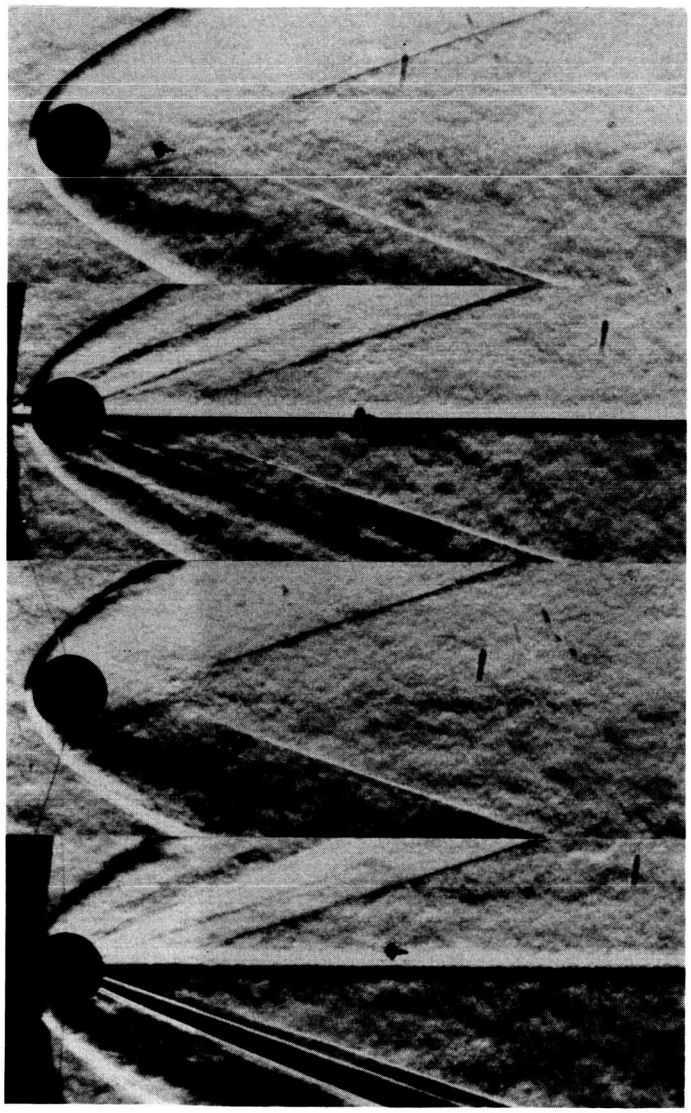

WIRE ORIENTATION	$\frac{L}{d}$
NO WIRE	1.22
HORIZONTAL	1.00
VERTICAL	0.98
HORIZONTAL AND VERTICAL	---

$M = 3$
SUPPLY PRESSURE ≅ 150 cm Hg
$R_D = 5.3 \times 10^5$
MODEL DIAMETER = $1\frac{1}{2}$ in.
WIRE DIAMETER = 0.020 In.

Fig. 20. Effect of support wire orientation on sphere wakes

VII. CONCLUSIONS

A. Model Wakes

The differences in wake characteristics of the cone models and those of the spheres are apparent in the spark schlieren photographs. In general, the intersection of the wake compression shock wave with the separation region is not as well defined for the cone models as for the spheres. For both classes of models, the wake shapes were strongly dependent upon both Mach and Reynolds numbers.

The wire supports had a considerable effect upon the sphere wakes at all Mach numbers tested. No effect of the wires upon the cone wakes was observable at $M = 2$ and below. As the Mach number increased, however, the effects of wire interference increased, and at $M = 4.7$ and 9, the effects were quite substantial. Any use of wires or other seemingly insignificant supports for wake studies, must be proven to be acceptable, as they can produce a noticeable wake effect.

B. Testing Techniques

The techniques used in conjunction with this Report are actually quite simple, and can easily be adapted for use in most wind tunnel facilities. During the JPL tests, two to three successful flights were normally made each hr, making it possible to obtain large amounts of such data in a relatively short period of time. The important point of this discussion is that it is conveniently practical to run extensive programs on the effects of Mach and Reynolds numbers and model shape and boundary layer upon wakes, as indicated by spark schlieren photographs.

Even when the flow densities are so low that the normal schlieren system is not sensitive enough to resolve the flow patterns in the wake region, visual observations of the wake shape can be made by ionizing the flow. By recording the data on film, it is practical to obtain flow-ionization wake data of free-flight models.

An additional advantage of this testing technique is the low acceleration ($< 10^2$ g's) that a model generally experiences. This makes it practical to perform wake studies on very delicate models such as those with relatively fine extension booms on the nose (separation spike) or on the base (for supporting instrumentation).

NOMENCLATURE

d	model diameter
L	length of separation region of sphere wake
L'	length of separation region of cone wake
M	Mach number
R_D	Reynolds number, based on freestream conditions and model diameter
r	radius of spherical tip on cone nose

REFERENCES

1. Dayman, B., Jr., *Simplified Free-Flight Testing in a Conventional Wind Tunnel,* Technical Report No. 32-346, Jet Propulsion Laboratory, Pasadena, October 1962.

2. Wind Tunnel Staff, *Wind Tunnel Facilities at the Jet Propulsion Laboratory,* Technical Report No. 34-257, Jet Propulsion Laboratory, Pasadena, January 1962.

3. Laufer, J., *Aerodynamic Noise in Supersonic Wind Tunnels,* Progress Report No. 20-378, Jet Propulsion Laboratory, Pasadena, February 1959.

4. Koester, E. H., J. J. Minich, and R. H. Lee, *Comments-on: 1) The Effects of Wall to Freestream Temperature Ratio on Boundary Layer Separation and 2) Use of Ionization for Flow Visualization in the JPL 21-Inch Hypersonic Wind Tunnel,* Internal Memorandum WT 21 T-57, Jet Propulsion Laboratory, Pasadena, September 1962.

5. Luther, M., *Fixing Boundary-Layer Transition on Supersonic-Wind-Tunnel Models (II),* Progress Report No. 20-287, Jet Propulsion Laboratory, Pasadena, February 1956.